

GENERATION OF GALVANIZED METAL IMAGES BY SKEWNESS

TORU HIRAOKA¹, HIROHUMI NONAKA² AND ELISA CLAIRE ALEMAN CARREON²

¹Department of Information Systems
University of Nagasaki
1-1-1, Manabino, Nagayo-chou, Nishisonogi-gun, Nagasaki-ken 851-2195, Japan
hiraoka@sun.ac.jp

²Department of Information and Management Systems Engineering
Nagaoka University of Technology
1603-1, Kamitomioka-chou, Nagaoka-shi, Niigata-ken 940-2188, Japan
{ nonaka; s153400 }@kjs.nagaokaut.ac.jp

Received April 2019; accepted July 2019

ABSTRACT. *We propose a non-photorealistic rendering method for generating galvanized metal images from gray-scale photographic images. Galvanized metal images are expressed by overlapping plated patterns of tin or aluminum on photographic images. Our method is executed by an iterative process using skewness. Our method has an advantage that galvanized metal patterns can be automatically generated according to the luminance of photographic images. In addition, our method can change the width and density of galvanized metal patterns by changing the values of the parameters. In order to verify the effectiveness of our method, we conducted experiments using various photographic images. As a result of the experiments, we clarified that the two advantages can be reproduced.*

Keywords: Non-photorealistic rendering, Galvanized metal, Skewness, Automatic generation

1. Introduction. Non-photorealistic rendering is processes of generating graphical images for display [1] from models by means of computer programs. Generation of non-photorealistic images has become popular in ACM SIGGRAPH since the 1990's [2, 3]. In recent years, researches have been carried out to generate non-photorealistic images by imitating patterns in nature or geometric patterns. Examples of such images are maze images [4], op-art images [5], pop-art images [6], reaction-diffusion-pattern images [7], cell images [8], concrete-wall images [9], and patchwork-stripe-art images [10]. Maze images were generated by creating stipplings from photographic images using centroidal Voronoi tessellation and then connecting all points in stipplings with minimum spanning trees. Op-art images were represented with densely packed line segments to depict simple shapes such as circles and squares. Pop-art images were generated using scalable vector graphics as a genotype representation in evolutionary art. Reaction-diffusion-pattern images were generated using anisotropic reaction diffusion introducing a flow field. Cell images were generated using inverse iris filter. Concrete-wall images were generated using autocorrelation coefficient and inverse filter. Patchwork-stripe-art images were generated using smoothing filter with four different window sizes. These images are utilized when artistic expression is required in magazines and websites, but more diverse artistic expressions are required.

In this paper, we develop a new process for generating galvanized metal images from gray-scale photographic images. Galvanized metal patterns express the change in gloss

that occurs in the smooth unevenness of plated metals such as tin and aluminum. Galvanized metal images are expressed by overlapping galvanized metal patterns on photographic images. To the authors' best knowledge, no previous research has studied the generation of galvanized metal images in non-photorealistic rendering.

Our method is executed by an iterative process using skewness, and has two features. The first feature is that galvanized metal patterns can be automatically generated according to the luminance of photographic images. The second feature is that the width and density of galvanized metal patterns can be changed according to the values of the parameters. In order to verify the effectiveness of our method, we conducted an experiment that examines how to form galvanized metal patterns when the values of the parameters are changed with Lenna image. In addition, we conducted an experiment using various photographic images other than Lenna image, and examined whether galvanized metal patterns can be automatically generated with all photographic images. As a result of the experiments, we clarified that our method can realize two features.

The rest of this paper is organized as follows. Section 2 describes our method for generating galvanized metal images. Section 3 shows experimental results, and reveals the effectiveness of our method. Finally, Section 4 concludes this paper.

2. Our Method. Our method generates galvanized metal images from gray-scale photographic images. Our method is executed in two processes. In the first process, skewness is calculated using the pixel values in the window. In the second process, images are converted using the skewness and photographic images. By repeating the two processes, galvanized metal images are generated. A flow chart of our method is shown in Figure 1.

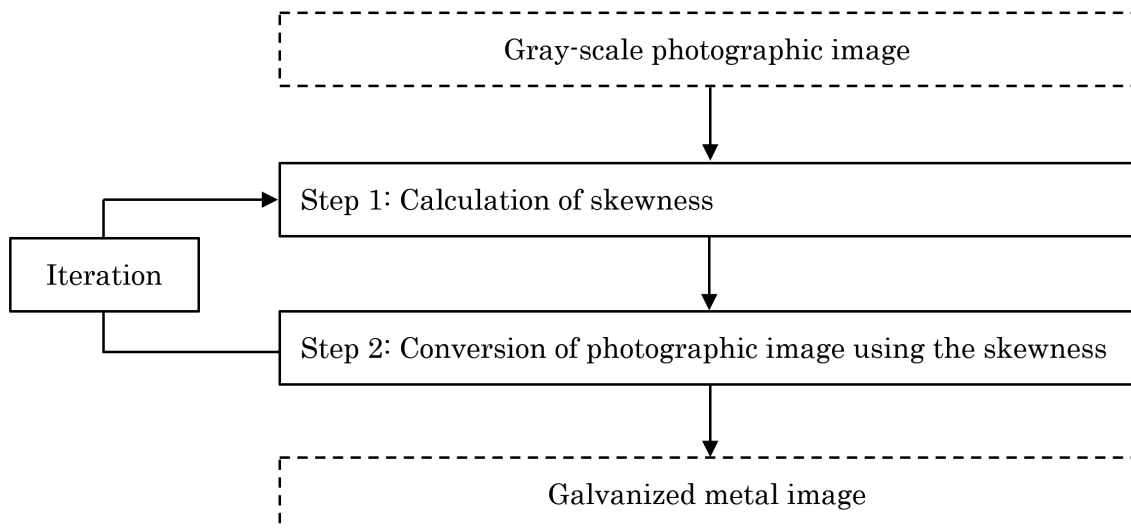


FIGURE 1. Flow chart of our method

The detailed procedure of our method is shown as follows.

Step 0: The input pixel values for spatial coordinates (i, j) of a gray-scale photographic image are defined as $f_{i,j}$. Then, the pixel values of the image at the t -th iteration number are defined as $f_{i,j}^{(t)}$, where $f_{i,j}^{(1)} = f_{i,j}$. In compliance with image data widely used in the world, the pixel values $f_{i,j}^{(t)}$ have value of 256 gradation from 0 to 255.

Step 1: Skewness $s_{i,j}^{(t)}$ of each pixel is calculated using the pixel values in the window of W pixels as the following equations.

$$a_{i,j}^{(t)} = \frac{\sum_{k=-W}^W \sum_{l=-W}^W \left(f_{i+k,j+l}^{(t)} - f_{i,j}^{(t)} \right)}{(2W + 1)^2} \quad (1)$$

$$s_{i,j}^{(t)} = \frac{\sum_{k=-W}^W \sum_{l=-W}^W \left(\left(f_{i+k,j+l}^{(t)} - f_{i,j}^{(t)} \right) - a_{i,j}^{(t)} \right)^3}{(2W + 1)^2} \quad (2)$$

where k and l are the positions in the window. In case $s_{i,j}^{(t)}$ is less than $-b$, then $s_{i,j}^{(t)}$ must be set to $-b$, where the threshold b is a positive constant. In case $s_{i,j}^{(t)}$ is greater than b , then $s_{i,j}^{(t)}$ must be set to b .

Step 2: The skewness $s_{i,j}^{(t)}$ is added to the pixel values $f_{i,j}$ of the photographic image, and the pixel values $f_{i,j}^{(t)}$ are updated to $f_{i,j}^{(t+1)}$ as the following equation.

$$f_{i,j}^{(t+1)} = f_{i,j} + s_{i,j}^{(t)} \quad (3)$$

In case $f_{i,j}^{(t+1)}$ is less than 0, then $f_{i,j}^{(t+1)}$ must be set to 0. In case $f_{i,j}^{(t+1)}$ is greater than 255, then $f_{i,j}^{(t+1)}$ must be set to 255. A galvanized metal image is obtained after the above processing of T times iteration.

3. Experiments. We mainly conducted two experiments. First, we conducted the experiment with changing the values of the parameters in the proposed method using Lenna image shown in Figure 2. Second, we conducted the experiment using various photographic images shown in Figure 3. All photographic images used in the experiments were $512 * 512$ pixels and 256 gradation.



FIGURE 2. Lenna image



FIGURE 3. Various photographic images

3.1. Experiment with changing parameters. Galvanized metal images by changing the iteration number T were visually confirmed using Lenna image. The iteration number T was set to 5, 10, 20, and 40. Other parameters W and b were set to 2 and 32, respectively. The results of the experiment are shown in Figure 4. As the value of the iteration number T was larger, galvanized metal patterns became clear and converged.

Galvanized metal images by changing the window size W were visually confirmed using Lenna image. The window size W was set to 1, 2, 3, and 4. Other parameters T and b

were set to 40 and 32, respectively. The results of the experiment are shown in Figure 5. As the value of the window size W was larger, the width of galvanized metal patterns became larger.

Galvanized metal images by changing the threshold b were visually confirmed using Lenna image. The threshold b was set to 16, 32, 48, and 64. Other parameters T and W were set to 40 and 2, respectively. The results of the experiment are shown in Figure 6. As the value of the threshold b was larger, the difference in brightness and darkness of galvanized metal patterns increased, and galvanized metal patterns were clearly expressed.

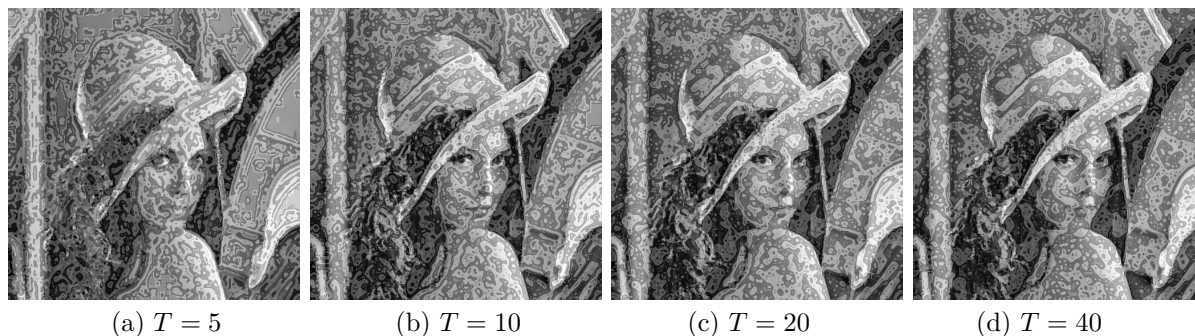


FIGURE 4. Galvanized metal images in the case of the iteration number $T = 5, 10, 20$, and 40

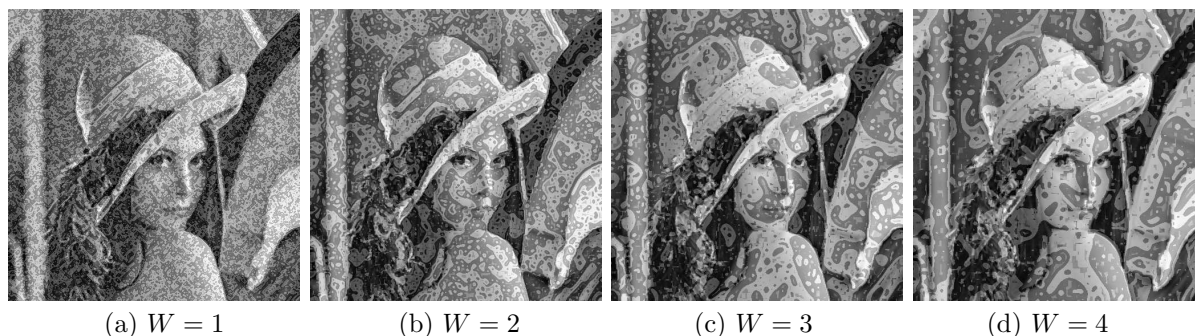


FIGURE 5. Galvanized metal images in the case of the window size $W = 1, 2, 3$, and 4

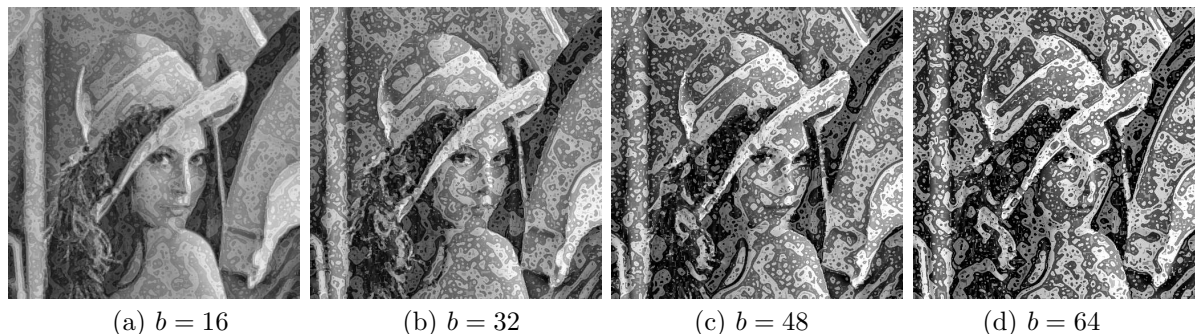


FIGURE 6. Galvanized metal images in the case of the threshold $b = 16, 32, 48$, and 64

3.2. Experiment using various photographic images. Our method was applied to four gray-scale photographic images shown in Figure 3. Since galvanized metal patterns and Lenna image were visually recognized well in the previous experiment, the parameters T , W , and b were set to 40, 2, and 32, respectively. The results of the experiment are shown in Figure 7. In all cases, galvanized metal patterns could be automatically generated on the whole image even in bright and dark areas. However, galvanized metal patterns were unlikely to occur in the fine-texture area as in the cliff portion of the galvanized metal image on the right end in Figure 7.



FIGURE 7. Galvanized metal images of photographic images in Figure 3

4. Conclusions. We proposed a non-photorealistic rendering method for generating galvanized metal images from gray-scale photographic images. Our method was executed by an iterative process using skewness. In order to verify the effectiveness of our method, we conducted experiments using various photographic images. As a result of the experiments, we revealed that galvanized metal patterns can be automatically generated according to the luminance of photographic images. In addition, we revealed that the width and density of galvanized metal patterns can be changed according to the values of the parameters.

A subject for future study is to expand our method in order to generate galvanized metal patterns in the area of the fine texture. Another task is to expand for applications to color photographic images and videos.

REFERENCES

- [1] M. Yang, H. Mei and D. Huang, An effective detection of satellite images via K-means clustering on Hadoop system, *International Journal of Innovative Computing, Information and Control*, vol.13, no.3, pp.1037-1046, 2017.
- [2] P. Haeberli, Paint by numbers: Abstract image representations, *ACM SIGGRAPH Computer Graphics*, vol.24, no.4, pp.207-214, 1990.
- [3] B. J. Meier, Painterly rendering for animation, *Proc. of ACM SIGGRAPH 1996*, pp.477-484, 1996.
- [4] K. Inoue and K. Urahama, Halftoning with minimum spanning trees and its application to maze-like images, *Computers & Graphics*, vol.33, no.5, pp.638-647, 2009.
- [5] T. C. Inglis, S. Inglis and C. S. Kaplan, Op art rendering with lines and curves, *Computers & Graphics*, vol.36, no.6, pp.607-621, 2012.
- [6] E. D. Heijer and A. E. Eiben, Evolving pop art using scalable vector graphics, *International Conference on Evolutionary and Biologically Inspired Music and Art*, pp.48-59, 2012.
- [7] M. T. Chi, W. C. Liu and S. H. Hsu, Image stylization using anisotropic reaction diffusion, *The Visual Computer*, vol.32, no.12, pp.1549-1561, 2016.
- [8] T. Hiraoka and M. Hirota, Generation of cell-like color animation by inverse iris filter, *ICIC Express Letters*, vol.12, no.1, pp.23-28, 2018.
- [9] T. Hiraoka, T. Katayama and K. Urahama, Generation of concrete-wall-texture-like images by autocorrelation coefficient and inverse filtering, *ICIC Express Letters*, vol.13, no.2, pp.127-132, 2019.
- [10] T. Hiraoka, H. Nonaka and Y. Tsurunari, Generation of patchwork-stripe-art images using smoothing filter with four different window sizes, *ICIC Express Letters*, vol.13, no.5, pp.375-380, 2019.